Bone Marrow-Derived Cells Promote Liver Regeneration in Mice With Erythropoietic Protoporphyria

María García-Bravo,[1,2,5] María-Josefa Morán-Jiménez,[1] Óscar Quintana-Bustamante,[2] Manuel Méndez,[1] Inmaculada Gutiérrez-Vera,[1] Juan Bueren,[2] Eduardo Salido,[3] José-Carlos Segovia,[2] Antonio Fontanellas,[4] and Rafael Enríquez de Salamanca[1]

Background. Bone marrow transplantation can reverse hepatic protoporphyrin accumulation and prevent the hepatobiliary complications characteristic of erythropoietic protoporphyria. The aim of this study was to assess the recruitment capacity of bone marrow cells in the damaged liver and their possible contribution to the improved or recovered hepatic function in a murine model of erythropoietic protoporphyria (EPP).

Methods. Lethally irradiated female EPP mice were transplanted with bone marrow cells from healthy male mice and were monitored during 12 or 36 weeks. Two groups of animals killed 12 weeks after transplant were also treated with granulocyte colony-stimulating factor.

Results. Cell transplantation decreased porphyrin contents in erythrocytes and liver. Improved hepatic structure and function and reduced hepatic fibrosis were observed, especially 36 weeks after transplant. Bone marrow-derived cells (22%–35%) were identified in the liver of recipient mice by means of fluorescence in situ hybridization (chrY-FISH) or green fluorescent protein staining and were characterized by immunofluorescence staining. The livers of recipients contained 20% to 30% myofibroblasts (α-smooth muscle actin-positive cells), 40% CK19-positive cells, and 10% to 28% hepatocytes (albumin-positive cells) derived from the donor bone marrow.

Conclusions. Bone marrow-derived cells play a significant role in restoring and regenerating hepatic tissue in EPP mice. Hepatic repair was associated with fibrogenesis, enhanced by granulocyte colony-stimulating factor treatment, and almost normal liver structure and function was observed in the long term (36 weeks posttransplant).

Keywords: Erythropoietic protoporphyria, Bone marrow-derived hepatocytes, Cell therapy, Liver regeneration, Liver repair.

Erythropoietic protoporphyria (EPP) is an inherited disease caused by the deficient activity of ferrochelatase (EC.4.99.1.1), the last enzyme in the heme biosynthetic pathway (*1*). Reduced ferrochelatase activity leads to the accumulation of protoporphyrin (PP) in erythrocytes, plasma, liver, and feces. The main clinical feature in EPP is skin photosensitivity resulting from the elevated levels of PP in circulating erythrocytes and plasma. Hepatic manifestations occur in approximately 20% of patients with EPP, and 5% to 10% of patients develop severe liver disease, with cholestasis, increased PP in the hepatocytes, macrophages, and bile canaliculi, fibrosis, and liver failure (*2*).

Currently, there is no effective therapy for EPP because photoprotection is ineffective in a proportion of patients and does not help to manage liver complications. In patients with hepatic cirrhosis, the only suitable therapy is liver transplant, but this treatment is not always available and the transplanted liver is also susceptible to PP-induced damage. Bone marrow transplantation is a potential candidate for therapy because it drastically reduces PP accumulation in erythrocytes and plasma and prevents cholestatic liver failure by reducing the biliary flow of hepatotoxic PP (3, 4). Two patients with EPP have undergone bone marrow transplantation to prevent recurrent hepatic complications after liver transplantation (5, 6).

Many studies have demonstrated the ability of hematopoietic stem cells (HSC) to generate functional cells of different nonhematopoietic tissues, pointing to possible regenerative medicine applications in rescuing the functionality of damaged tissues (7, 8). This property of HSC has been termed cell plasticity. Although in most studies plasticity seems as a rare event, the conversion of HSC into different tissues has been demonstrated (e.g., hepatocytes, endothelial cells, skeletal muscle fibers, cardiomyocytes, neural cells, and renal tubular epithelial cells) (9–13).

Tutois et al. have developed a mouse model of EPP in which homozygous mutant mice show a 95% reduction in ferrochelatase activity. EPP mice develop photosensitivity, jaundice, hemolytic anemia, cholestasis, and severe liver dysfunction at an early age (14). Previous studies have used this mouse model to demonstrate the long-term cure of cutaneous lesions by bone marrow transplantation of wild-type cells or gene therapy-corrected cells (15–17).

It has been demonstrated that when both the replication from mature hepatocytes and progenitor cells are blocked, as occurs in the livers of transplanted mice because of the toxic effect of PP, bone marrow cells can generate these cells (18). On the basis of these data, HSC have been suggested as a source of hepatocyte recruitment for EPP liver regeneration. Hematopoietic growth factors regulate the proliferation and differentiation of hematopoietic cells (19, 20), and granulocyte colony-stimulating factor (G-CSF) has been shown to significantly enhance the generation of bone marrow-derived hepatocytes in models of hepatic injury (21).

The aims of this study were to verify the existence of cells of donor origin in the liver of $Fech^{m1Pas}/Fech^{m1Pas}$ mice after bone marrow transplantation with normal bone marrow cells, to characterize these cells, and to examine their contribution to improving the hepatopathy in this model. We also examined whether treatment with the hematopoietic progenitor mobilization factor G-CSF increases the number of hepatic cells of donor origin in the livers of recipient mice and improves liver regeneration.

MATERIALS AND METHODS

Animal Model and Bone Marrow Transplantation

$Fech^{m1Pas/m1Pas}$ mice (BALB/cJ) (EPP mice) were obtained from the Jackson Laboratory (Bar Harbor, ME). All mice were kept under pathogen-free conditions in air-filtered cages and provided with an autoclaved food and water. The mice had unlimited access to water and standard laboratory feed and were subjected to 12-hr light/dark cycles. All animal experiments were conducted in accordance with European Council Guidelines (86/609 EEC, 90/67 EEC, 99/575 EEC) and the Spanish Royal Decree 1201/2005. Eight weeks-old female recipient mice were transfused through a lateral tail vein with 10^7 nucleated bone marrow cells obtained by flushing femoral and tibial bones of wild-type male donors with a 25-gauge needle containing phosphate-buffered saline. Recipient mice were lethally irradiated using a Philips MG324 X-ray equipment (Philips, Hamburg, Germany) to deliver two doses, 24 hr apart, of 4.75 Gy, 300 kV and 12.8 mA at a dose rate of 1.03 Gy/min.

Five different groups of animals ($n=5$–7 each) were established (Fig. 1a): wild-type mice ($+/+$) killed at 16 weeks of age (group 1); EPP mice ($-/-$) killed at 16 weeks of age (group 2); EPP female mice grafted with bone marrow cells from wild-type male mice and killed 12 weeks after transplant (group 3); EPP female mice grafted with bone marrow cells from wild-type male mice and killed 12 weeks after transplant and 3 weeks after G-CSF treatment (group 4), and EPP female mice grafted with bone marrow cells from wild-type male mice and killed 36 weeks after transplant (group 5). As an alternative method for identifying donor cells, bone marrow cells from healthy transgenic mice expressing the enhanced green fluorescent protein (EGFP) under the control of a β-actin promoter were transplanted in EPP female; animals were killed 12 weeks after transplant and 3 weeks after G-CSF treatment.

Hematopoietic Cell Mobilization

For G-CSF treatment, 50 μg/mouse of pegylated G-CSF (Neulasta, Amgen, Breda, The Netherlands) in phosphate-buffered saline/0.1% bovine serum albumin was administered by subcutaneous injection once a week for 3 weeks (Fig. 1a). Mice were killed 3 weeks after the last injection.

Hematological and Biochemical Measurements

Blood parameters were measured using standard methods (Technicon H-11 System). The plasma biochemical variables normally determined, total bilirubin, transaminases, and alkaline phosphatase, were estimated by standard methods (Beckman Synchron CX7, Beckman Instruments, Brea, CA).

Ferrochelatase Activity and Porphyrin Levels

Hepatic ferrochelatase activity was determined by the method described by Camadro and Labbe (22), consisting of fluorimetric measurement of zinc-PP formed after incubation of liver homogenates with zinc and PP. Porphyrin concentrations in plasma, erythrocytes, and liver were determined spectrofluorimetrically (Shimadzu RF-1501, Germany) according to the previously described methods (23, 24).

Liver Histology and Immunohistological Analysis

Histological analysis of the livers of control and recipient mice was carried out on 5-μm paraffin-embedded sections. Hematoxylin-eosin and Masson's trichrome were used to determine structure and fibrosis, respectively. Slides were analyzed by a trained pathologist, who was blind to the origin of the sections, to evaluate lesions following the criteria described elsewhere (2).

To identify activated myofibroblasts, sections were immunostained for α-smooth muscle actin (α-sma) (mouse monoclonal Clone 1A4 labeled with Cy3, Sigma, Saint Louis,
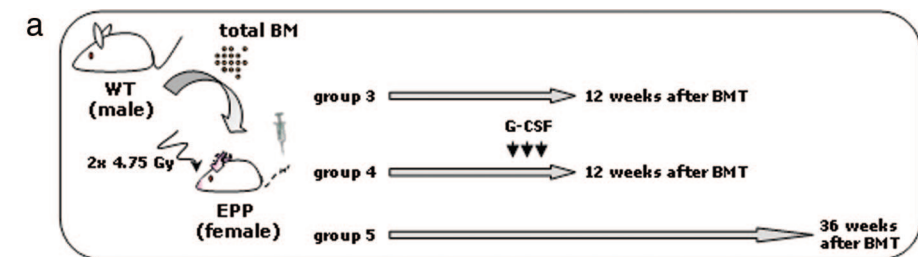
FIGURE 1. (a) Experimental design. All animals were transplanted at 8 weeks of age. Mice in groups 3 and 4 were killed 12 weeks after transplantation and, respectively, did not or did receive granulocyte-colony stimulating factor (G-CSF) treatment. Animals in group 5 were killed 36 weeks after transplant. Hematoxylin-eosin staining of liver tissue from (b) wild-type (WT) mice and (c) erythropoietic protoporphyria (EPP) mice; *arrows* show deposits of protoporphyrin (PP) in the lumen of bile ducts. (d) Masson's trichrome staining of the liver tissue from animals in group 4, killed 12 weeks after transplant, showed periportal fibrosis and porto-portal bridges. (e) Hematoxylin-eosin staining of liver tissue from mice in group 3 showed an atypical ductular reaction around portal tracks. (f) Hematoxylin-eosin staining of the liver tissue from animals in group 4. *Arrow* shows deposits of PP in the lumen of bile ducts, distension, and proliferation of bile ducts. (g) Hematoxylin-eosin staining showed minor PP deposits and improve in hepatic architecture 36 weeks posttransplant. BM, bone marrow; BMT, bone marrow transplant.
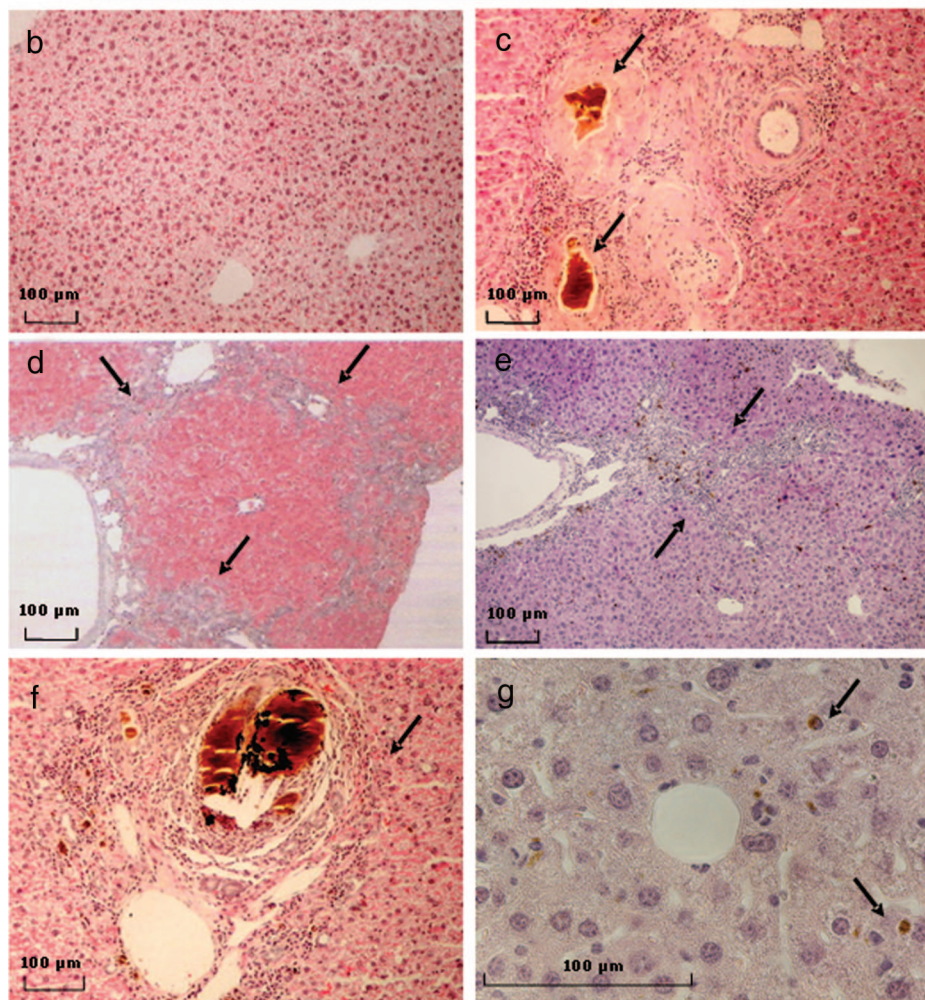
MO; working dilution 1:100). Hepatocytes were characterized by staining albumin with a sheep anti-mouse albumin antibody as the primary antibody (Biogenesis Ltd., UK; working dilution 1:100) and a donkey anti-sheep IgG antibody labeled with Alexa Fluor 594 as the secondary antibody (Molecular Probes Inc., Spain; working dilution 1:250). To discriminate infiltrated hematopoietic cells in the livers of recipient mice, liver sections were immunostained with a rat anti-mouse CD45 antibody (AbD Serotec, Bionova Científica SL, Spain; working dilution 1:100); a rabbit anti-rat IgG antibody labeled with Cy3 was used as the secondary antibody (Sigma, Saint Louis, MO; working dilution 1:600). The oval reaction was identified using a rabbit anti-mouse cytokeratin 19 antibody (Novus Biologicals, Bionova Científica, Spain; working dilution 1:50); the secondary antibody used was a donkey anti-rabbit IgG antibody conjugated to Alexa Fluor 594 (working dilution 1:100).

As an alternative method for tracing of donor cells, sections were immunostained for GFP (rabbit anti-GFP, Molecular Probes Inc., Spain; working dilution 1:100); a donkey anti-rabbit IgG antibody labeled with Alexa Fluor 488 was used as the secondary antibody (Molecular Probes Inc., Spain; working dilution 1:1000).

For liver fibrosis determination, liver sections were stained with 0.1% picrosirius red for image analysis quantification. Picrosirius red stains connective fibers a deep red and cell nuclei and cytoplasm structures a light red/bright yellow.

Fluorescent In Situ Hybridization

The bone marrow origin of liver cells was checked by fluorescent in situ hybridization (FISH) using a specific probe for the murine Y chromosome according to the manufacturer's instructions (Cambio, Cambridge, UK). FISH was per-

formed on tissue sections that had been previously subjected to immunohistochemistry and were counterstained and mounted using Vectashield containing DAPI (Vector Laboratories, Burlingame, CA) to identify cell nuclei.

Chimerism was also characterized by FISH of bone marrow cells from recipient animals using the same mouse Y chromosome-specific probe (Cambio).

Microscopy and Image Capture

Liver tissue sections were analyzed by digitally photographing 10 random fields using the 40×/0.75 Nikon Plan Fluor objective of a Nikon Eclipse TE2000-S microscope. To quantify the Y chromosome, a correction factor was determined in liver sections of male mice because some Y chromosomes could be overlooked. CorelDRAW Graphics Suite software was used to process the combined images of immunostaining and FISH. Confocal images were captured using a Leica TCS SPE microscope.

Percentage of fibrosis was estimated in 17 random images taken in two nonconsecutive sections stained for picrosirius red. The total collagen content of liver sections was quantified by computer-assisted image analysis at the Morphology and Imaging Unit (CIMA, Pamplona, Spain). Data were acquired using an automatic macro developed under Metamorph Imaging software (Molecular Devices, Inc. Toronto, Canada). The image analysis software was developed using MATLAB v.7.1.0 and DIPlib v1.5.0 C libraries under OS Red Hat Linux AS 2.6.9-11.

Statistical Analysis

The nonparametric Mann-Whitney test was used for comparison between two groups and Spearman's rank correlation was used to assess corelationships. The level of significance was set at P less than 0.05. Quantitative data were expressed as means±standard deviation. All statistical tests were performed using the program GraphPad Prism 4.00 for Windows (GraphPad Software, San Diego, CA; www.graphpad.com).

RESULTS

Porphyrin Levels in Blood and Liver and Hepatic Ferrochelatase Activity Are Partly Recovered After Bone Marrow Transplantation

We evaluated the chimerism of transplanted mice by conducting Y-FISH on bone marrow cells because recipient and donor mice were females and males, respectively. After applying a correction factor of 1.434, because of the sensitivity of the technique, chimerism in bone marrow ranged from 71.7% to 107% (see *Material and Methods*).

To check whether metabolic correction had occurred, we monitored porphyrin levels in blood and liver (Table 1). Twelve weeks after transplant, normal erythrocyte PP contents were restored in all the groups of bone marrow transplanted mice, and plasma porphyrin levels were drastically reduced from 70-fold to 2-fold wild-type levels. Twelve weeks after transplant, hepatic PP contents fell to one half the contents recorded in nontransplanted EPP mice, although these differences failed to reach significance. At 36 weeks of transplant, PP levels were 10 times lower than the amounts observed in EPP mice ($P<0.01$). Animals treated with G-CSF (group 4) showed a lower drop in hepatic porphyrin concentrations compared with groups 3 and 5. Ferrochelatase activity in the livers of EPP mice was 9.7% normal values. Transplanted animals analyzed 12 weeks after transplant (groups 3 and 4) showed similar liver ferrochelatase activities to EPP mice. Thirty-six weeks after transplant (group 5), this activity was significantly higher, up to 20% the activity recorded in healthy controls (Table 1).

TABLE 1. Plasma and erythrocyte porphyrin levels 8 wk after BMT

Group	BMT (treatment) (sacrifice age) (wk)	Recipient mice	n	Porphyrins level			Hepatic ferrochelatase activity (nmol PROTO-Zn/hr/g prot)
				Plasma (nmol porphyrins/L)	RBC (nmol PROTO/g Hb)	Liver (nmol PROTO/g prot)	
1	No (16)	+/+	6	70.03±10.88	4.99±0.90	89±24	1.781±0.169
2	No (16)	EPP	6	4822±3783	94.33±30.52	10985±3758	0.173±0.021
				$P<0.05$ (2 vs. 1)	$P<0.05$ (2 vs. 1)	$P<0.01$ (2 vs. 1)	$P<0.005$ (2 vs. 1)
3	+/+ male (20)	EPP female	5	179.4±65.18	4.06±0.64	5764±4817	0.205±0.088
				$P<0.05$ (3 vs. 1)	NS (3 vs. 1)	$P<0.05$ (3 vs. 1)	$P<0.005$ (3 vs. 1)
				$P<0.05$ (3 vs. 2)	$P<0.05$ (3 vs. 2)	NS (3 vs. 2)	NS (3 vs. 2)
4	+/+ male (G-CSF) (20)	EPP female	6	184.7±36.36	4.18±0.80	8588±3318	0.212±0.053
				$P<0.01$ (4 vs. 1)	NS (4 vs. 1)	$P<0.01$ (4 vs. 1)	$P<0.005$ (4 vs. 1)
				$P<0.01$ (4 vs. 2)	$P<0.01$ (4 vs. 2)	NS (4 vs. 2)	NS (4 vs. 2)
						NS (4 vs. 3)	NS (4 vs. 3)
5	+/+ male (44)	EPP female	7	147±31.2	5.6±2.04	989±801	0.345±0.102
				$P<0.01$ (5 vs. 1)	NS (5 vs. 1)	$P<0.01$ (5 vs. 1)	$P<0.005$ (5 vs. 1)
				$P<0.01$ (5 vs. 2)	$P<0.01$ (5 vs. 2)	$P<0.01$ (5 vs. 2)	$P<0.005$ (5 vs. 2)
						$P<0.05$ (5 vs. 3)	NS (5 vs. 3)

Porphyrins levels and ferrochelatase activity in liver at time of sacrifice. Age at the moment of transplantation: 8 wk.
BMT, bone marrow transplantation; G-CSF, granulocyte colony-stimulating factor; EPP, erythropoietic protoporphyria; RBC, red blood cells; NS, not significant.

TABLE 2. Plasma biochemical parameters of control and cellular therapy groups at time of sacrifice

| Group	BMT (treatment) (sacrifice age) (wk)	Recipient mice	n	AST (UI/L)	ALT (UI/L)	Alkaline phosphatase (UI/L)	Total bilirubin (mg/dL)
1	No (16)	+/+	6	79±16	63±15	378±92	0.059±0.021
2	No (16)	EPP	6	665±213	483±162	1141±259	2.424±0.499
				$P<0.01$ (2 vs. 1)	$P<0.01$ (2 vs. 1)	$P<0.01$ (2 vs. 1)	$P<0.01$ (2 vs. 1)
3	+/+ male (20)	EPP female	5	415±109	314±126	725±154	0.054±0.011
				$P<0.01$ (3 vs. 1)	$P<0.01$ (3 vs. 1)	$P<0.01$ (3 vs. 1)	NS (3 vs. 1)
				NS (3 vs. 2)	NS (3 vs. 2)	$P<0.05$ (3 vs. 2)	$P<0.01$ (3 vs. 2)
4	+/+ male (G-CSF) (20)	EPP female	6	740±695	400±125	955±447	0.052±0.058
				$P<0.01$ (4 vs. 1)	$P<0.01$ (4 vs. 1)	$P<0.01$ (4 vs. 1)	NS (4 vs. 1)
				NS (4 vs. 2)	NS (4 vs. 2)	NS (4 vs. 2)	$P<0.01$ (4 vs. 2)
				NS (4 vs. 3)	NS (4 vs. 3)	NS (4 vs. 3)	NS (4 vs. 3)
5	+/+ male (44)	EPP female	7	232±71	192±120	691±138	0.246±0.141
				$P<0.005$ (5 vs. 1)	$P<0.01$ (5 vs. 1)	$P<0.01$ (5 vs. 1)	$P<0.005$ (5 vs. 1)
				$P<0.005$ (5 vs. 2)	$P<0.05$ (5 vs. 2)	$P<0.05$ (5 vs. 2)	$P<0.005$ (5 vs. 2)
				$P<0.05$ (5 vs. 3)	NS (5 vs. 3)	NS (5 vs. 3)	$P<0.005$ (5 vs. 3)

Age at the moment of transplantation: 8 wk.

BMT, bone marrow transplantation; EPP, erythropoietic protoporphyria; ALT, alanine aminotransferase; AST, aspartate aminotransferase; NS, not significant.

Bone Marrow Transplant Leads to the Partial Recovery of Liver Function and Partial Reversal of Histological Alterations in the Liver

Levels of aspartate aminotransferase, alanine aminotransferase, and alkaline phosphatase were all elevated in the EPP mice. After bone marrow transplant, levels of both transaminases and alkaline phosphatase were intermediate between those detected in the healthy and EPP animals, although this recovery was greater 36 weeks after bone marrow transplant (group 5) than after 12 weeks (groups 3 and 4). Serum bilirubin was increased 40-fold in the EPP mice, falling by 95% (groups 3 and 4) and 90% (group 5) after bone marrow transplant (Table 2).

We also examined the histological characteristics of the liver in the control groups and in all transplanted mice. Macroscopically, the livers of EPP mice were easily distinguished by their dark color and nodular surface. Hematoxylin-eosin staining revealed the presence of Councilman bodies and dark brown pigment, especially in bile ducts, and the altered architecture of liver tissue, which showed inflammatory infiltrates in portal tracts sometimes expanding to the parenchyma (Fig. 1c). The lumen of most large bile ducts was distended and filled with PP deposits, and small bile ducts proliferated around them (Fig. 1c). Masson's trichrome staining revealed portal and periportal fibrosis, and in groups 3 and 4 some areas were identified as regenerative nodules (Fig. 1d). Mice killed 12 weeks after transplant (group 3) showed a similar hepatic architecture to EPP mice. A quantitative study of fibrosis by sirius red staining indicated a discrete reduction in the extent of fibrosis observed in the hepatic parenchyma of animals in group 3 (4.2% vs. 5.6% in EPP mice) (Fig. 2f). Interestingly, 36 weeks after transplant, the mice in group 5 showed a normal liver architecture, minor hepatocellular damage, small deposits of PP, normal bile ducts, and marked reduction in fibrosis (2.8% vs. 4.2% in group 3) (Figs. 1g and 2e–f). Histological analysis revealed
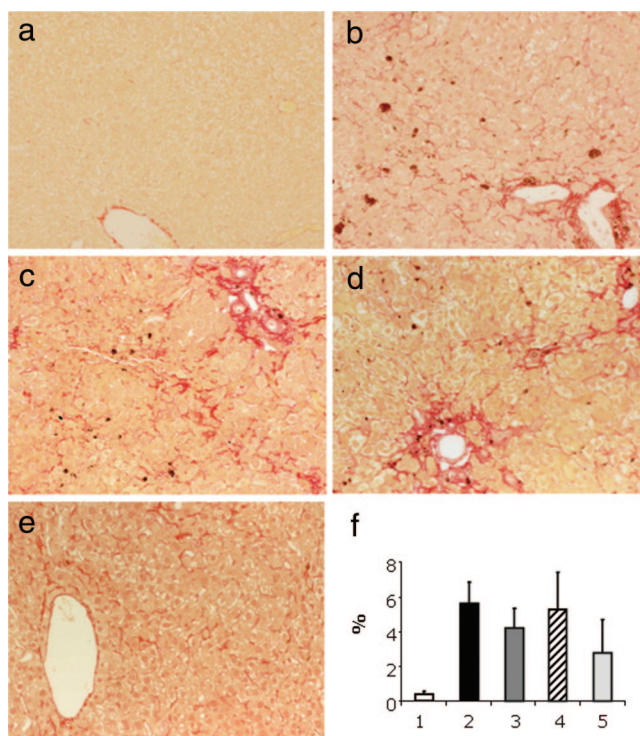
FIGURE 2. Sirius red staining (connective fibers, deep red) of liver parenchyma in wild-type mice (a), erythropoietic protoporphyria (EPP) mice (b), animals killed 12 weeks after transplant not given and given granulocyte-colony stimulating factor (G-CSF) treatment (c–d) and animals killed 36 weeks after transplant (e). Percent collagen-producing cells in the liver of all the experimental groups (f).

high intragroup heterogeneity, although the mice treated with G-CSF (group 4) displayed more PP deposits, more inflammatory infiltrates, greater distension and proliferation of bile ducts, and more profuse fibrosis, including bridging

fibrosis, as shown in our quantitative analysis of fibrosis (5.3% vs. 4.2% in group 3) (Figs. 1d and 2d, f). Similar results were obtained in the semiquantitative assessment of fibrosis conducted on Masson's trichrome-stained sections.

Donor Bone Marrow Cells Contribute to Liver Repair and Liver Regeneration in EPP Mice After Bone Marrow Transplantation

The presence of Y chromosome-positive cells indicating their donor animal bone marrow origin was estimated in the liver of all the groups of transplanted mice by the FISH technique as: 26.3%±7.8% in group 3, 22.3%±7.0% in group 4, and 34.7%±15.5% in group 5. No statistically significant differences existed among groups. These results were confirmed by EGFP staining of the liver from animals transplanted with EGFP-expressing bone marrow cells: 21% of the liver cells were originated from donor cells in this group. By characterizing the Y chromosome-positive cells using specific tissue markers, we were able to obtain more information on the functionality of the donor-derived cells in the liver. Hematopoietic cells were identified by staining for CD45. In all three groups of transplanted mice, HCS accounted for approximately 10% of the total number of hepatic cells and appeared near blood vessels. Approximately 60% of these CD45-positive cells were Y chromosome positive, indicating a slight repopulation by a small number of endogenous hematopoietic cells in these animals. Albumin staining revealed the existence of bone marrow-derived hepatocytes in the livers of recipient mice. Among all the albumin-positive cells detected, 12 weeks after transplant (group 3), 11% were Y chromosome/albumin double-positive cells and this percentage increased to 17% of hepatocytes 36 weeks after transplant ($P<0.01$ group 5 vs. group 3) (Figs. 3a and 4). After treatment with G-CSF, 28% of hepatocytes from male donor origin were observed in the livers of mice killed 12 weeks after transplant ($P<0.01$, group 4 vs. group 3). Alternative detection of bone marrow-derived hepatocytes was performed by double staining for EGFP and albumin in liver sections from animals
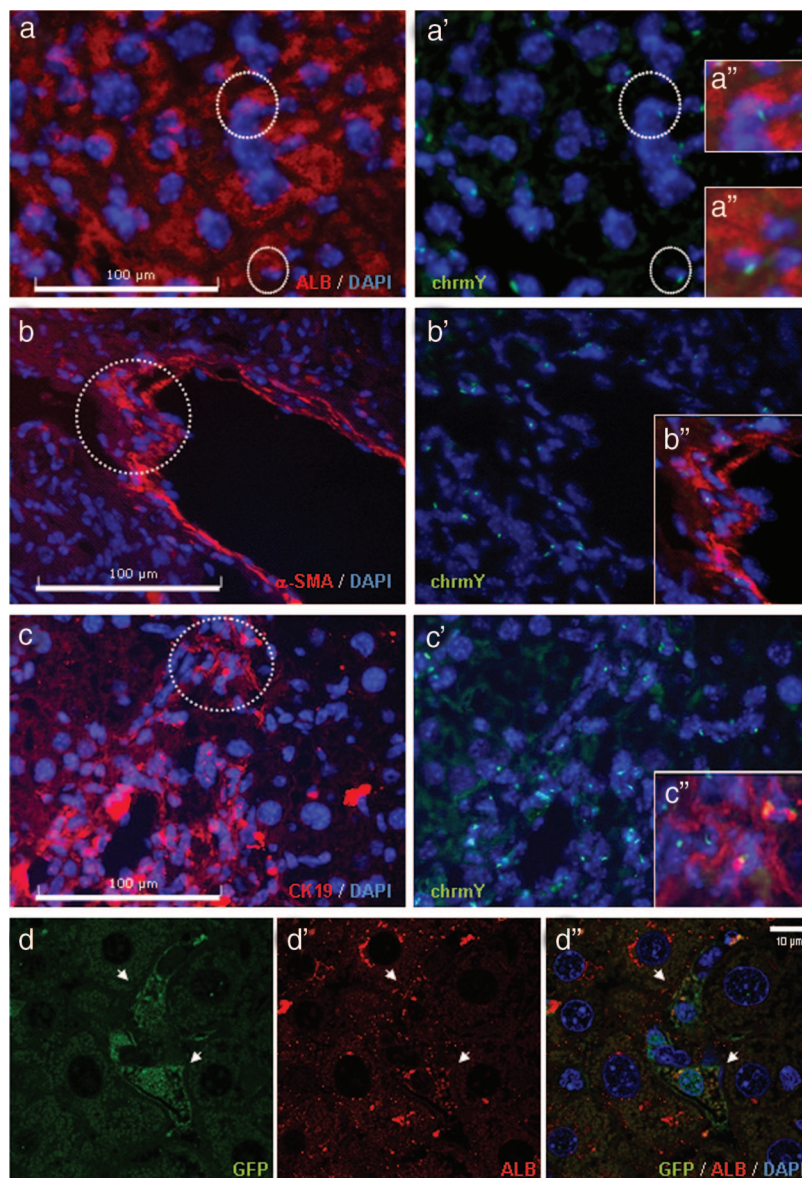
FIGURE 3. Bone marrow-derived cells (chromosome Y-positive cells, green) co-expressing (a) albumin (red), (b) α-sma (red), or (c) cytokeratin 19 (CK19) in the liver tissue from transplanted erythropoietic protoporphyria (EPP) mice. Circled: some double-positive cells. (a″, b″, c″) Circled double-positive cells enlarged. (d) Confocal microscopy of two bone marrow-derived hepatocytes. Green fluorescent protein (GFP) (green) and albumin (red) colocalize in the same cell.
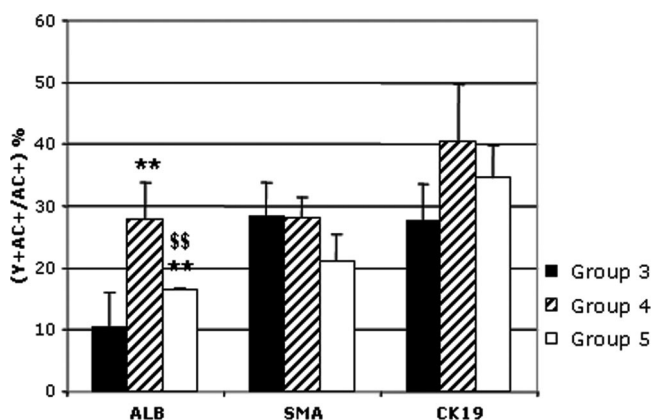
FIGURE 4. Percentages of hepatocytes (albumin-positive cells), myofibroblasts (α-sma-positive cells), and CK19-positive cells that were bone marrow-derived (Y-chromosome/marker double positive cells) in the transplant groups. (**$P<0.01$, vs. group 3; $\$\$P<0.01$, vs. group 3).

transplanted with EGFP-expressing bone marrow cells (Fig. 3d). Percentage of bone marrow-derived hepatocytes (EGFP/albumin double-positive cells) detected by this method was approximately 15% of total hepatocytes (albumin-positive cells).

To check that the bone marrow cells were indeed contributing to liver repair and regeneration, we determined relative amounts of donor and recipient origin α-sma-positive and CK 19-positive cells. In the liver of control mice, α-sma-positive cells were only around vessels, however, in transplanted EPP mice up to 30% of myofibroblasts (α-sma-positive cells) were Y chromosome positive at 12 weeks posttransplant (groups 3 and 4). Thirty-six weeks after transplant (group 5), this proportion fell to 20%, although the difference was not significant (Figs. 3b and 4).

In the liver of EPP transplanted mice, an atypical ductular reaction was observed near α-sma-positive cells, at the interface with and around portal tracks. Most of the liver cells of donor bone marrow origin were positive for CK19 staining (Fig. 3c). Remarkably, up to 27% and 34% of these cells were of donor origin (Y chromosome/CK 19 double-positive cells) 12 and 36 weeks after transplant, respectively; and this figure rose to 40% after treatment with G-CSF (Fig. 4).

DISCUSSION

The only established treatment of liver failure is allogenic liver transplant, which is limited by the availability of donor organs. Among the other options under investigation, cell therapy with isolated hepatocytes could be the most promising, however, current techniques need to be adapted to increase the yield and quality of the final grafted hepatocytes (25). The use of adult stem cells might be a suitable alternative for cell transplantation; these cells have the properties of self-renewal and a capacity to differentiate into different types of specialized cells, depending on the microenvironment. The Fech^{m1Pas}/Fech^{m1Pas} mutant mouse is a good model of liver failure (3, 26). It shows increased PP levels, cholestasis, and severe liver dysfunction at an early age similar to that reported in patients with EPP, and this feature makes it a suitable model for chronic hepatic disease. In previous studies, it has been reported that

bone marrow transplantation in the Fech$^{m1Pas/m1Pas}$ model is able to rescue the cutaneous manifestation of the disease by correcting the erythropoietic alterations of EPP (26).

Chronic liver damage induces a regenerative process and given this condition is successfully reproduced, this model is ideal for examining the recruitment of bone marrow stem cells in the damaged liver and their possible contribution to improving or recovering hepatic function and regeneration. In this study, after having observed correction of erythropoietic alterations, we wanted to determine whether further replacement of EPP bone marrow with healthy bone marrow cells might contribute to improving hepatic function through the recruitment of bone marrow stem cells to the liver of recipient mice.

We observed here that PP concentrations in red blood cells were reduced to normal levels in transplanted mice attributable to the high chimerism observed in the bone marrow of these animals. Plasma porphyrin concentrations were reduced approximately 30-fold compared with the levels detected in EPP mice. Twelve weeks after transplant, porphyrin concentrations in the liver corresponded to 53% of the concentrations observed in the EPP animals and 78% after G-CSF treatment. These results are similar to those observed 24 weeks after transplant and previously described (26) and indicate the erythropoietic origin of most of the porphyrin that builds up in the liver of EPP mice. Interestingly, 36 weeks posttransplant the EPP recipients showed scarce PP accumulation and reduced PP levels when compared with mice tested 12 weeks after transplant. This more marked decrease in hepatic porphyrin in group 5 could suggest that in the long term the liver recovers the ability to excrete excess of PP.

Because cell therapy was directed at the bone marrow, we did not expect the activity of hepatic ferrochelatase to be corrected, as indeed we observed in animals undergoing bone marrow transplant that were killed 12 weeks later (groups 3 and 4). However, 36 weeks after transplant (group 5), hepatic ferrochelatase activity increased twofold with respect to basal values. This increased activity of ferrochelatase could be due to the contribution of the bone marrow-derived cells (BMDCs) nested in the liver, although not correlation was found between percentage of BMDCs and the increase in the activity of ferrochelatase.

The impaired liver function indicated by the biochemical variables determined in the EPP mice showed a trend toward improvement after the transplant of healthy bone marrow. Our results indicate that this improvement was modulated by time because transaminases and alkaline phosphatase showed greater reductions in the group examined 36 weeks after transplant. Remarkably, normal bilirubin levels were restored 12 weeks after transplant. Conversely, G-CSF treatment rendered no improvement in hepatic function over that observed in animals killed at the same time (Table 2).

The liver has a tremendous capacity for self-regeneration through compensatory growth, and the usual mode of liver regeneration and repair involves the replication of mature hepatocytes (27). However, cytotoxic bile containing a high concentration of PP and bile salts is believed to cause damage and loss of hepatocytes and epithelial cells from bile ducts (4). This could give rise to an atypical ductular reaction because oval cells are known to be activated and to proliferate only when endogenous hepatocytes are blocked (27). In effect, the activation and proliferation of oval cells have been described

in this mouse model of EPP (*2*) and we observed an atypical ductular reaction, as occur in patients, in the EPP mouse model.

This atypical reaction was localized in portal areas and their interface and consisted of arboreal strands of oval cells immunoreactive for cytokeratin 19 (Fig. 1e). The mice in group 5, killed 36 weeks after transplant, only showed discrete areas staining for cytokeratin 19 and a reduced number of regenerative nodules, both associated with decreased α-fetoprotein concentrations in liver homogenates (data not shown). These findings could indicate some degree of reversal or remission in the long term of the hepatocarcinogenesis process reported in this mouse model (*2*). The increase in CK19-positive cells derived from the bone marrow, most likely oval cells, which could mean an oval cell reaction process, was greater in animals treated with G-CSF, in which CK19-positive cells represented close to 50% of the total number of hepatic cells, than in the other groups of transplanted mice. We detected a large percentage of bone marrow-derived CK19-positive cells, as indicated by their double positivity for CK19 and the Y chromosome. Up to 40% of the CK19-positive cells in group 4 were of donor origin.

These results suggest that most of the BMDCs identified in the EPP livers contribute to hepatic regeneration through the activation and proliferation of hepatic progenitor cells. A recent study conducted in a murine model of oval cells activation reported that following bone marrow transplantation, up to 20% of oval cells expressed donor markers. The authors suggest that when endogenous oval cells are inhibited a second population from bone marrow is recruited to the liver to help promote hepatic regeneration (*18*).

In this study, we noticed a significant percentage of bone marrow-derived hepatocytes after transplant. Recent studies have tried to determine whether transplanted bone marrow stem cells are able to generate hepatocytes in both healthy and injured livers. So far, results indicate that bone marrow cells have a minimal capacity to generate hepatocytes in normal livers and a low capacity in injured livers. The exception is the production of hepatocytes of bone marrow origin in fumarylacetoacetate hydrolase knockout mice, as a consequence of cell fusion (*8*). Interestingly, no clear oval cell reaction is observed in the fumarylacetoacetate hydrolase model. Given that a high number of oval cells arise from the bone marrow, it can be assumed that some, if not all, bone marrow-derived hepatocytes observed were the product of the differentiation of bone marrow-derived oval cells. Currently, we are engaged in in vivo fusion experiments to address whether other mechanisms of bone marrow-derived hepatocyte generation are also taking place.

In this EPP mouse model, we observed high percentages of bone marrow-derived hepatocytes after transplant. Approximately 10% of the examined hepatocytes (albumin-positive cells) were donor derived (albumin and Y chromosome double positive) 12 weeks after transplant. This proportion rose significantly to 28%, after treatment with G-CSF. Approximately 15% of bone marrow-derived hepatocytes were identified by double immunostaining (albumin/GFP) in the livers from animals transplanted with EGFP-expressing bone marrow cells. Lower percentage of bone marrow-derived hepatocytes obtained in this group compared with group 4 could be due to the fact that only approximately 60% of hepatocytes from

transgenic mice were positive for GFP staining in donor animals (*28*) and also because of the lower sensibility of GFP staining versus FISH detection. In group 5, 17% of hepatocytes were donor derived 36 weeks after transplant. The high proportions of bone marrow-derived hepatocytes in groups 4 and 5 point to positive effects of G-CSF or time in the regenerative process through hepatocyte generation after bone marrow transplant.

Myofibroblasts (α-sma-positive cells) are distributed cells involved in growth, differentiation, development, and repair during the inflammatory response and their overactivation leads to fibrotic diseases, including hepatic fibrosis (*29*). Our histological study and quantification of collagen deposits revealed portal and periportal fibrosis in the livers of EPP mice. We also detected occasional foci of steatosis and necrotic hepatocytes. Deposits of PP were found in canaliculi, bile ducts, and Kupffer cells. These findings are in agreement with those reported by others in this mouse model of porphyria (*2, 14*). The dark PP deposits observed in liver sections from transplanted EPP mice were reduced in all the transplant groups compared with amount of PP deposits in the liver from EPP control mice, although the reduction was most evident 36 weeks after transplant (Table 1). These findings are also consistent with the greater recovery observed in serum liver function tests and with our previously reported data (*26*) and are related to the improved liver structure and reduced size of fibrotic areas, especially in the long-term transplant group (Figs. 1g and 2e–f).

We also evaluated the contribution of recruited donor-origin cells to hepatic fibrosis after bone marrow transplant in EPP mice. Wide areas immunoreactive for α-sma were detected, mainly in portal areas and surrounding hepatic nodules. This distribution concurs with the results obtained using the trichrome and sirius red stains. The proportions of myofibroblasts of donor origin observed in EPP mice after bone marrow transplantation were approximately 20% to 25% of the total number of myofibroblasts in all the transplant groups (Fig. 4). Thirty-six weeks after transplant, histological analysis revealed a recovered hepatic tissue and α-sma immunostaining confirmed the lower number of cells contributing to hepatic fibrosis. Moreover, through digital image analysis a significant decrease in the collagen content of the liver was detected in EPP animals in this group (Fig. 2e–f).

In conclusion, in this EPP mouse model, we were able to detect a high percentage of BMDCs implanted in the liver of recipient mice. These cells of donor origin contribute to processes of hepatic repair and regeneration through the generation of myofibroblasts, hepatocytes, and CK19-positive cells. Treatment with G-CSF increased the contribution of the bone marrow to liver cells, including myofibroblasts. Accordingly, treatment with G-CSF is not recommended in liver diseases with established fibrosis. Moreover, it should be noted that the recipient mice in this study were 8 weeks, with established hepatic disease. Thus, we would expect both compromised hepatocyte proliferation and enhanced liver regeneration through the proliferation of oval cells. This indicates the need in patients with a high risk of developing liver disease to perform bone marrow transplant before liver damage spreads, when the hepatic parenchyma still has the capacity for liver regeneration without having to resort to hepatic progenitors. Finally, a sufficient length of time after cell

transplant is needed to restore liver structure and function, including diminished fibrosis.

REFERENCES

1. Anderson KE, Sassa S, Bishop DF, et al. Disorders of heme biosynthesis: X-linked sideroblastic anemia and the porphyrias. In: Scriver CR, Beaudet al, Sly WS, et al, eds. The metabolic and molecular bases of inherited diseases. New York, Mc Graw Hill 2001, p. 2991.
2. Libbrecht L, Meerman L, Kuipers F, et al. Liver pathology and hepatocarcinogenesis in a long-term mouse model of erythropoietic protoporphyria. *J Pathol* 2003; 199: 191.
3. Abitbol M, Bernex F, Puy H, et al. A mouse model provides evidence that genetic background modulates anemia and liver injury in erythropoietic protoporphyria. *Am J Physiol Gastrointest Liver Physiol* 2005; 288: G1208.
4. Meerman L, Koopen NR, Bloks V, et al. Biliary fibrosis associated with altered bile composition in a mouse model of erythropoietic protoporphyria. *Gastroenterology* 1999; 117: 696.
5. Rand EB, Bunin N, Cochran W, et al. Sequential liver and bone marrow transplantation for treatment of erythropoietic protoporphyria. *Pediatrics* 2006; 118: 1896.
6. Wahlin S, Aschan J, Björnstedt M, et al. Curative bone marrow transplantation in erythropoietic protoporphyria after reversal of severe cholestasis. *J Hepatol* 2007; 46: 174.
7. Masson S, Harrison DJ, Plevris JN, et al. Potential of hematopoietic stem cell therapy in hepatology: A critical review. *Stem Cells* 2004; 22: 897.
8. Thorgeirsson SS, Grisham JW. Hematopoietic cells as hepatocyte stem cells: A critical review of the evidence. *Hepatology* 2006; 43: 2.
9. Abedi M, Greer DA, Colvin GA, et al. Robust conversion of marrow cells to skeletal muscle with formation of marrow-derived muscle cell colonies: A multifactorial process. *Exp Hematol* 2004; 32: 426.
10. Jang YY, Collector MI, Baylin SB, et al. Hematopoietic stem cells convert into liver cells within days without fusion. *Nat Cell Biol* 2004; 6: 532.
11. Krause DS, Theise ND, Collector MI, et al. Multi-organ, multi-lineage engraftment by a single bone marrow-derived stem cell. *Cell* 2001; 105: 369.
12. Lagasse E, Connors H, Al-Dhalimy M, et al. Purified hematopoietic stem cells can differentiate into hepatocytes in vivo. *Nat Med* 2000; 6: 1229.
13. Theise ND, Badve S, Saxena R, et al. Derivation of hepatocytes from bone marrow cells in mice after radiation-induced myeloablation. *Hepatology* 2000; 31: 235.
14. Tutois S, Montagutelli X, Da Silva V, et al. Erythropoietic protoporphyria in the house mouse. A recessive inherited ferrochelatase deficiency with anemia, photosensitivity, and liver disease. *J Clin Invest* 1991; 88: 1730.
15. Pawliuk R, Bachelot T, Wise RJ, et al. Long-term cure of the photosensitivity of murine erythropoietic protoporphyria by preselective gene therapy. *Nat Med* 1999; 5: 768.
16. Fontanellas A, Mendez M, Mazurier F, et al. Successful therapeutic effect in a mouse model of erythropoietic protoporphyria by partial genetic correction and fluorescence-based selection of hematopoietic cells. *Gene Ther* 2001; 8: 618.
17. Richard E, Mendez M, Mazurier F, et al. Gene therapy of a mouse model of protoporphyria with a self-inactivating erythroid-specific lentiviral vector without preselection. *Mol Ther* 2001; 4: 331.
18. Oh SH, Witek RP, Bae SH, et al. Bone marrow-derived hepatic oval cells differentiate into hepatocytes in 2-acetylaminofluorene/partial hepatectomy-induced liver regeneration. *Gastroenterology* 2007; 132: 1077.
19. De Silvestro G, Vicarioto M, Donadel C, et al. Mobilization of peripheral blood hematopoietic stem cells following liver resection surgery. *Hepatogastroenterology* 2004; 51: 805.
20. Yannaki E, Athanasiou E, Xagorari A, et al. G-CSF-primed hematopoietic stem cells or G-CSF per se accelerate recovery and improve survival after liver injury, predominantly by promoting endogenous repair programs. *Exp Hematol* 2005; 33: 108.
21. Quintana-Bustamante O, Alvarez-Barrientos A, Kofman AV, et al. Hematopoietic mobilization in mice increases the presence of bone marrow-derived hepatocytes via in vivo cell fusion. *Hepatology* 2006; 43: 108.
22. Camadro JM, Labbe P. Purification and properties of ferrochelatase from the yeast *Saccharomyces cerevisiae*. Evidence for a precursor form of the protein. *J Biol Chem* 1988; 263: 11675.
23. Piomelli S. Free erythrocyte porphyrins in the detection of undue absorption of Pb and of Fe deficiency. *Clin Chem* 1977; 23: 264.
24. Grandchamp B, Deybach JC, Grelier M, et al. Studies of porphyrin synthesis in fibroblasts of patients with congenital erythropoietic porphyria and one patient with homozygous coproporphyria. *Biochim Biophys Acta* 1980; 629: 577.
25. Taléns-Visconti R, Bonora-Centelles A, Castell JV, et al. Alternative sources of hepatocytes for cell therapy. *Gastroenterol Hepatol* 2006; 29: 366.
26. Fontanellas A, Mazurier F, Landry M, et al. Reversion of hepatobiliary alterations by bone marrow transplantation in a murine model of erythropoietic protoporphyria. *Hepatology* 2000; 32: 73.
27. Fausto N. Liver regeneration and repair: Hepatocytes, progenitor cells, and stem cells. *Hepatology* 2004; 39: 1477.
28. Swenson ES, Price JG, Brazelton T, et al. Limitations of green fluorescent protein as a cell lineage marker. *Stem Cells* 2007; 25: 2593.
29. Forbes SJ, Russo FP, Rey V, et al. A significant proportion of myofibroblasts are of bone marrow origin in human liver fibrosis. *Gastroenterology* 2004; 126: 955.